Effect of the cold-drawing process on fatigue behaviour of V-shaped notched round bars

Andrea Carpinteri, Roberto Brighenti, Andrea Spagnoli, Sabrina Vantadori

Dept. of Civil-Environmental Engineering & Architecture, Univ. of Parma, Viale Usberti 181/A, 43100 Parma, Italy; Fax: +39 0521 905924; E-mail: sabrina.vantadori@unipr.it

ABSTRACT. *The state of stress in a structural component is generally influenced by both service loadings and mechanical effects due to production processes, such as residual stresses generated by inhomogeneous plastic deformations. Sometimes the effect of residual stresses on the mechanical and fatigue properties is beneficial, sometimes it is detrimental. Since the component failure can be caused by both applied and residual stresses, it is important to understand the role of residual stresses. In the present paper the effect of residual stresses, due to the cold-drawing process, on the fatigue behaviour of a metallic cracked round bar with a V-shaped circumferential notch is examined. The stress-intensity factors related to tension loading and to a residual stress field are numerically evaluated. Then, the crack propagation under cyclic tension is analysed through a theoretical model, by also including the effect of residual stresses. Such an effect is taken into account considering, for some values of residual stress severity, the actual stress ratio which is different from the nominal one due to cyclic tension only.*

INTRODUCTION

Generally speaking, the stress field in a structural component is caused by both service loadings and manufacturing processes. The stresses due to such processes, called residual stresses, are usually due to inhomogeneous plastic deformations produced by mechanical, thermic or chemical phenomena [1], and have a significant effect on the fatigue behaviour of structures. Furthermore, the effect of possible stress concentrators, which can modify the stress field, has to be taken into account.

Several authors have examined the fatigue behaviour of notched bars under different loading conditions [2-5], but only few studies have analysed the influence of the residual stresses [6, 7].

In the present paper, a cold-drawn round bar with a V-shaped circumferential notch (Fig. 1) is subjected to pulsating tension. The axisymmetrical profile of the residual stress is numerically determined in the reduced cross-section of the bar (S-S in Fig. 1b), where an almond surface crack is assumed to exist. The stress-intensity factors (SIFs) due to residual stresses and tensile loading are evaluated by employing: a 3-D FE model, the power series expansion of the stress field, the superposition principle.

Then, the effect of the residual stresses on the fatigue behaviour of such a notched bar is examined. The actual stress ratio, evaluated by taking into account both the tensile

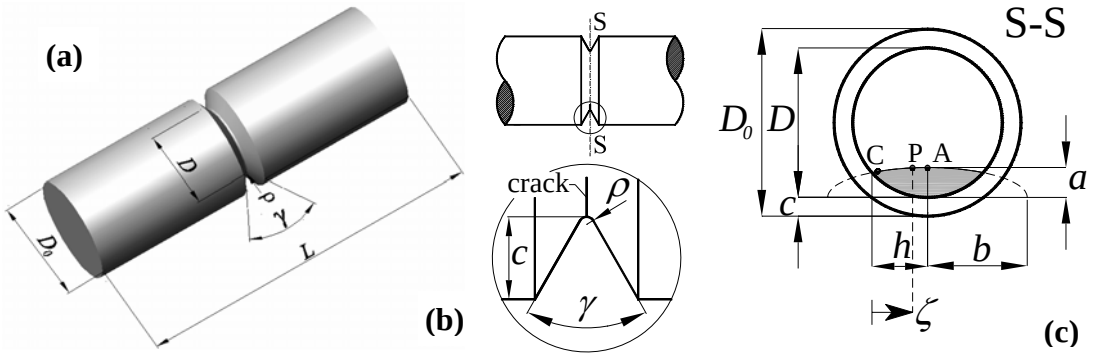

Figure 1. (a) 3-D view of the round bar with a circumferential notch. (b) Geometrical details of the V-shaped notch profile. (c) Geometrical parameters of the surface crack assumed in the reduced cross-section S-S.

stresses and the residual stresses, shows a non-uniform distribution on the crack front. The influence of the actual stress ratio on the fatigue crack propagation is considered by using the Walker equation [8], and the strong dependence of the propagation process on the residual stress field is quantified in terms of evolution of both surface crack shape and crack growth rate.

DEFINITION OF THE PROBLEM

The structural component being examined is a round bar with a V-shaped circumferential notch (Fig. 1) characterized by a depth c, an opening angle γ, a constant notch root radius ρ (Fig. 1b). The diameter of the bar is equal to D_0 in an unnotched cross-section and equal to D in the reduced cross-section S-S (Fig. 1b). The relative notch depth $\delta = c/D_0$ and the dimensionless notch root radius $\rho_d = \rho/D_0$ are assumed to be equal to 0.2 (i.e. $D = 0.6\ D_0$) and 0.009, respectively, whereas the opening angle γ is equal to $60°$.

The stress concentration factor (SCF) under tension, determined through a finite element analysis, is equal to $K_{t,F} = 6.13$, which is in a good agreement with the value $K_{t,F} = 6.01$ obtained by Noda e Takase [9]. An almond surface crack with an elliptical-arc shape is assumed to exist at the notch root (Fig. 1c). The crack configuration is characterized by the relative crack depth $\xi = a/D$ of the deepest point A and by the flaw aspect ratio $\alpha = a/b$. In the following, ξ is made to vary from 0.1 to 0.7, whereas the parameter α ranges from 0.0 to 1.2. The generic point P along the crack front is identified by the dimensionless coordinate $\zeta^* = \zeta/h$ (Fig. 1c).

The structural component is assumed to be subjected to an axisymmetrical residual stress field, due to cold-drawing process. Such a stress field, found out in numerical and experimental observations [10-13], is produced by pulling the bar through a die.

COLD-DRAWING RESIDUAL STRESSES

The longitudinal residual stress data for an *unnotched bar* ($\rho_d = \infty$), determined by Elices [13] through the neutron and X-ray diffraction technique, are shown by solid symbols in Fig. 2a, where the radial coordinate r is normalized with respect to the bar radius R_0 (i.e. $r^* = r / R_0$) and the residual stress with respect to the residual stress value at the bar centre (i.e. $\sigma^*_{I(res)} = \sigma_{I(res)} \,/\, \sigma_{I(res)}(r=0)$). By interpolating such data through a best fitting polynomial, a continuous curve is obtained (Fig. 2a).

Such an axisymmetrical stress distribution has been used to numerically assess the residual stress distribution in a *notched bar* ($\rho_d = 0.009$). The dimensionless residual stress profile, in correspondence to the reduced section S-S, is reported in Fig. 2b (in such a case, the dimensionless radial coordinate is given by $r^* = r / R$).

A generic axysimmetrical residual stress distribution given by

$$\sigma_{I(res)}(r) = \sigma_{I(res)}(r=0) \cdot \sigma^*_{I(res)}(r) \tag{1}$$

can be approximated through a power series expansion as follows:

$$\sigma_{I(res)}(r) \cong \sum_{i=0}^{n} \frac{1}{i!}\left(\frac{d^{(i)}\sigma_{I(res)}(r)}{dr^{(i)}}\right)_{r=0} \cdot r^i = \sum_{i=0}^{n} A_{i(res)} \cdot r^i = \sum_{i=0}^{n} B_{i(res)} \cdot (r^*)^i \tag{2}$$

where r^* is given by $r / \overline{R}$ ($\overline{R}$ is equal to R_0 for unnotched bar and to R for notched bar), and the coefficients $B_{i(res)}$ are expressed by the following equation:

$$B_{i(res)} = \overline{R}^i \left[\frac{1}{i!}\left(\frac{d^{(i)}\sigma_{I(res)}(r)}{dr^{(i)}}\right)_{r=0}\right] = \sigma_{I(res)}(0) \cdot B^*_{i(res)} \quad \text{with} \quad B^*_{i(res)} = \frac{\overline{R}^i}{i!}\left[d^{(i)}\sigma^*_{I(res)} / dr\right]_{r=0} \tag{3}$$

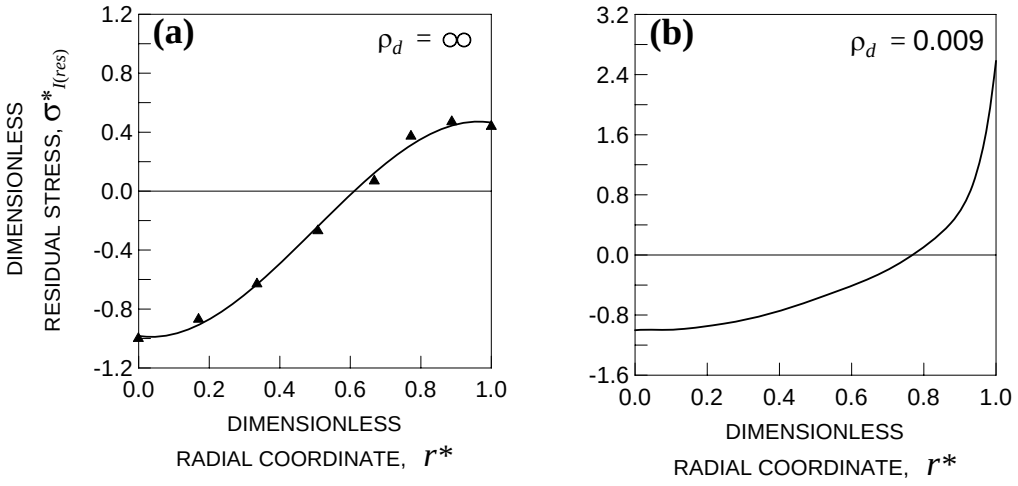

Figure. 2. Dimensionless residual stress distribution $\sigma^*_{I(res)}$ against dimensionless radial coordinate r^* : (a) unnotched round bar; (b) notched round bar.

Different residual stress distributions are hereafter considered, by assuming the above stress patterns (Fig. 2) and varying the value of $\sigma_{I(res)}(0)$. Their effects are quantified in term of SIF, and their influence on the fatigue behaviour is examined.

RESIDUAL STRESS INFLUENCE ON SIFS AND ON STRESS RATIO

In order to evaluate the SIF produced by a generic longitudinal residual stress distribution, the SIFs ($K_{I(i)}$) related to elementary stress distributions ($\sigma_{I(i)} = (r^*)^i$, i = 0,...,n) acting on the crack faces are computed along the crack front and properly combined [14]. Such SIFs are evaluated by means of the quarter-point finite element nodal displacement correlation technique [15,16]. In a dimensionless form, they can be written as $K^*_{I(i)} = K_{I(i)} / \sqrt{\pi \cdot a}$.

A generic complex axisymmetrical stress distribution $\sigma_{I(L)}(r)$, perpendicular to the crack faces, can be approximated through a power series expansion as has been done for the residual stress (Eq. (2)), and the corresponding polynomial coefficients $B_{i(L)}$ can be determined by applying Eq. (3_1) to $\sigma_{I(L)}(r)$.

Since the superposition principle holds, the dimensionless SIFs corresponding to such a complex load distribution and to residual stresses can be approximated as [14]:

$$K^*_{I(L)} \cong \frac{1}{\sigma_{ref(L)}} \sum_{i=0}^{n} \sigma_{ref(i)} B_{i(L)} K^*_{I(i)}, \qquad K^*_{I(res)} \cong \frac{1}{\sigma_{I(res)}(0)} \sum_{i=0}^{n} \sigma_{ref(i)} \cdot B_{i(res)} K^*_{I(i)} \quad (4)$$

By defining the residual stress severity as $s = \sigma_{I(res)}(0) / \sigma_{ref(F)}$ where the subscript (F) indicates tension loading, the residual stress influence on the dimensionless total SIF, given by $K^*_{I(F+res)} = (K_{I(F)} + K_{I(res)}) / \sigma_{ref(F)} \sqrt{\pi a}$, can be appreciated, as is shown in Fig. 3. In such a figure, the values of $K^*_{I(F+res)}$ at point A and point C on the crack front are plotted against the relative crack depth ξ ($0.1 \le \xi \le 0.5$), for a straight- and a circular-fronted crack, by assuming s equal to 0.0 (pure tension), 0.5, 1.0.

For unnotched bar with straight-fronted crack (Fig. 3a), the dimensionless SIF at point C increases by increasing the residual stress severity s. At point A, it increases only for small values of the relative crack depth ($\xi \le 0.4$): for ξ greater than 0.4, the influence of residual stresses becomes negligible. For unnotched bar with circular-arc crack (Fig. 3b), the dimensionless SIF at point C increases by increasing the residual stress severity s, whereas the dimensionless SIF at point A can increase or decrease with the relative crack depth: as a matter of fact, a transition value of ξ, approximately equal to 0.3, can be observed.

For notched bar (Fig. 3c and 3d), the dimensionless SIF at point C increases with the residual stress severity s. On the other hand, by increasing s, the dimensionless SIF at

point A increases for $\xi < 0.3$ in the case of straight-fronted crack (Fig. 3c) and for $\xi < 0.2$ in the case of circular-arc crack (Fig. 3d).

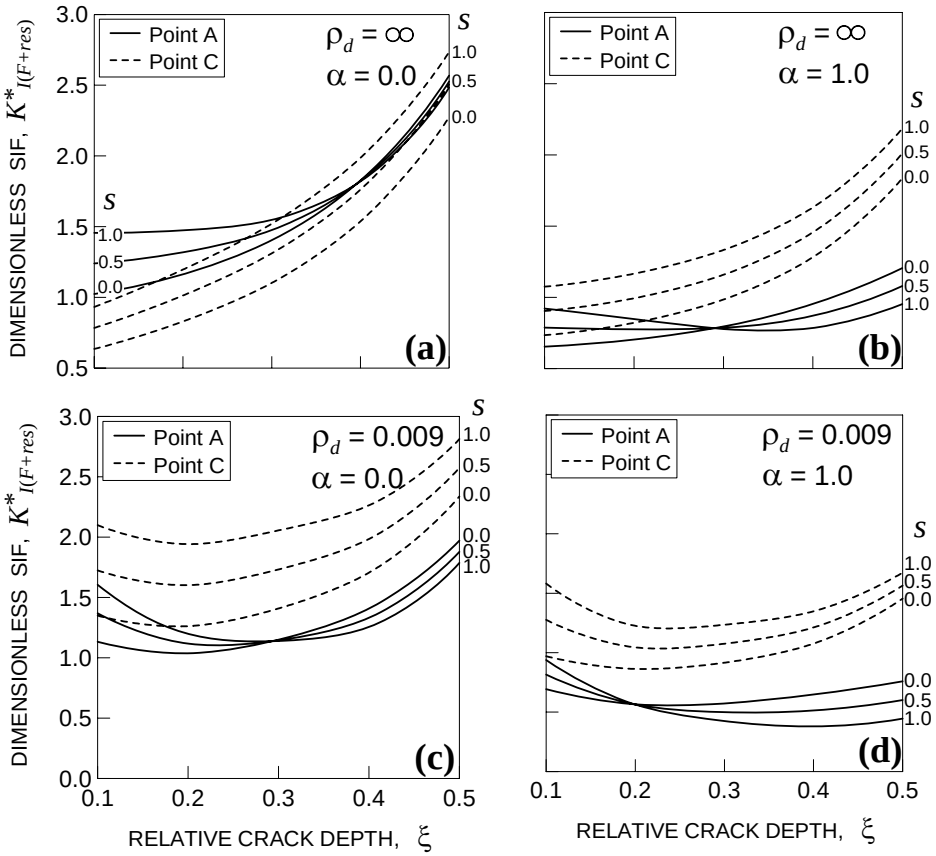

Figure 3. Dimensionless total stress-intensity factor $K^*_{I(F+res)}$ against relative crack depth ξ, for different values of s: (a, b) unnotched round bar and (c, d) notched round bar; (a, c) straight-fronted crack and (b, d) circular-arc fronted crack.

From the above discussion, it can be deduced that the effect of the residual stresses on the SIFs is remarkable and, therefore, a significant change of the fatigue behaviour of both unnotched and notched bars can also be expected by varying the value of the parameter s. Since the present paper aims at investigating the effect of different residual stress distributions on the fatigue behaviour of round bars under constant amplitude cyclic tension, the actual stress ratio R_a needs to be evaluated:

$$R_a(r) = \left[R_F + s \cdot \sigma^*_{I(res)}(r)\right] / \left[1 + s \cdot \sigma^*_{I(res)}(r)\right] \tag{5}$$

where R_F is the nominal stress ratio of the cyclic tension, i.e. $R_F = \sigma_{(F)\min} / \sigma_{(F)\max}$, and $\sigma_{ref(F)}$ in s (see just after Eq.(4)) is assumed to be equal to the maximum stress $\sigma_{(F)\max}$.

In Fig. 4, the actual stress ratio R_a is plotted against the dimensionless radial coordinate r^*. For both unnotched (Fig. 4a) and notched (Fig. 4b) bar, by increasing the parameter s the actual stress ratio R_a increases in the outside part of the bar and decreases in the inner part of the bar.

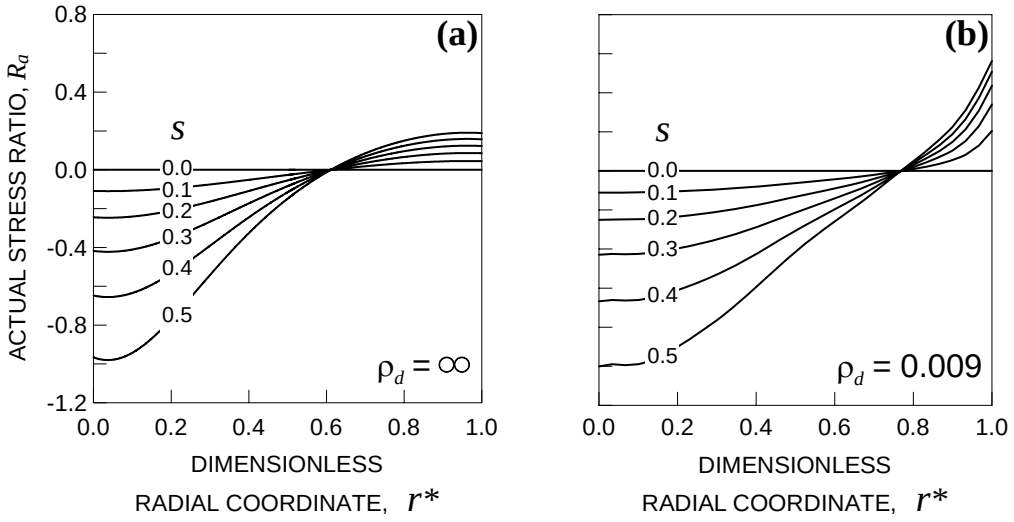

Figure 4. Actual stress ratio R_a against radial coordinate r^*, for different values of s and cyclic tension with $R_F = 0.0$: (a) unnotched round bar; (b) notched round bar.

FATIGUE CRACK PROPAGATION

Now the fatigue behaviour under tension loading is examined through a two-parameter theoretical model [15], by also using the Paris-Erdogan equation [17] modified by means of the Walker relationship [8]. It has experimentally been observed [18] that the coefficient C of the Paris-Erdogan equation is not only dependent on the material, but also on the stress ratio of the applied cyclic loading. Many equations have been proposed to take into account the stress ratio effect [8, 19-21]. The empirical Walker equation modifies the Paris-Erdogan law as follows [8, 22]:

$$da/dN = \overline{C}(R_L)\cdot\left[\Delta K_I\right]^m \quad \text{with} \quad \overline{C}(R_L) = C_0\left(1-R_L\right)^{-(1-\beta)m} \tag{6}$$

where $\overline{C}(R_L)$ is the effective Paris-Erdogan coefficient for a generic stress ratio R_L, C_0 is $\overline{C}(R_L)$ for R_L = 0, and β is the Walker exponent. It has been found that, for positive stress ratio values, the exponent β usually ranges from 0.3 to 0.8 ($\beta = 0.3$ and $\beta = 0.8$ produce a strong and a weak dependence on R_L, respectively). For negative stress ratio values, β can be set equal to zero because only $K_{I\,(\max)}$ drives the crack [22].

The parameters C_0 and m are here assumed equal to $1.64\cdot10^{-10}$ and 2 (with da/dN in $[\mathrm{mm}\cdot\mathrm{cycle}^{-1}]$ and ΔK_I in $[\mathrm{N}\cdot\mathrm{mm}^{-3/2}]$) [23], and the exponent β equal to 0.5.

The diagrams of crack aspect ratio α against relative crack depth ξ are determined for two initial crack configurations, $\sigma_{(F)\max}$ = 100 MPa, R_F = 0.0. For unnotched ($\rho_d = \infty$, Fig. 5a) and notched ($\rho_d = 0.009$, Fig.5b) bars, by increasing the residual stresses the curves tend to lower values of α for a given value of ξ. A remarkable dependence of the crack paths on the parameter s can be observed.

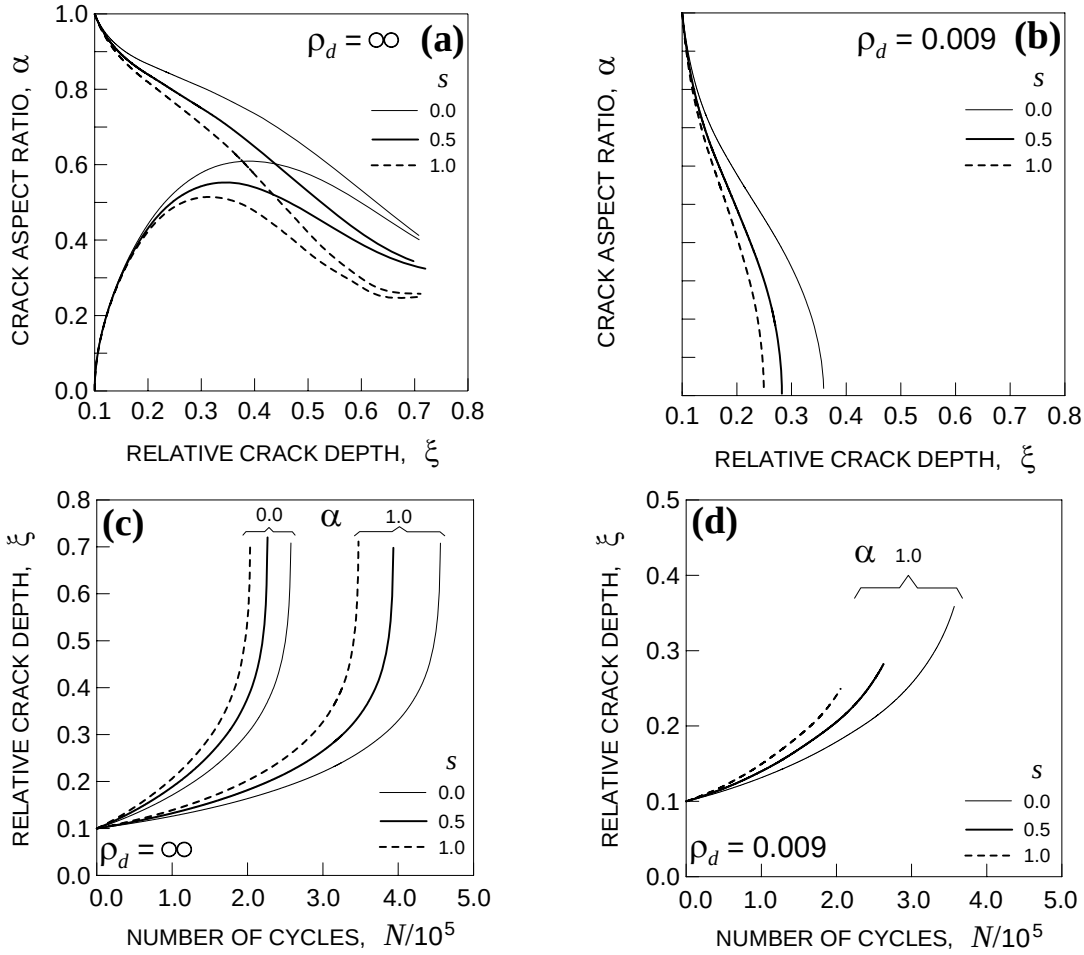

Figure 5. Crack aspect ratio α against relative crack depth ξ (a, b) and relative crack depth ξ against number of cycles N (c, d) in the case of unnotched bar (a, c) and notched bar (b, d) under cyclic tension, for two initial cracks and different values of s.

Note that, in the case of notched bars (Fig. 5b), only the curves related to $\alpha = 1.0$ are reported. As a matter of fact, cracks with an initial crack aspect ratio equal to 0.0 tend to assume a sickle shape just after a low number of loading cycles.

The crack depth evolution against the number of loading cycles is displayed in Fig.5. For unnotched (Fig. 5c) and notched (Fig. 5d) bar, the surface crack grows more rapidly in the case of high values of the residual stress severity s.

CONCLUSIONS

In the present paper, the effect of residual stresses due to cold-drawing process on the fatigue behaviour of a metallic notched round bar with a surface crack has been examined. Different residual stress distributions have been considered, and the bar has been assumed to be also subjected to cyclic tension. The fatigue crack propagation has been analysed by using the Walker equation, in order to take into account the effect of the actual stress ratio.

It has been observed that the residual stress field appreciably influences both the crack aspect ratio evolution and the crack growth rate. In particular, the residual stresses being examined tend to accelerate the crack propagation phenomenon in the case of both unnotched and notched bars.

REFERENCES

1. Bhadeshia, H.K.D.H. (2002) In: Handbook of residual stress and deformation of steel (Edited by Totten G., Howes M. and Inoue T.) pp. 3-10 ASM International.
2. Caspers, M., Mattheck C. and Munz D. (1990) ASTM STP pp. 365-389, 1060.
3. Lin X.B. and Smith R.A. (1999) Int. J. Fat. **21**: 965-973
4. Carpinteri A., Brighenti R. and Vantadori S. (2006) Int. J. Fat. **28**: 251-260
5. Carpinteri A., Vantadori S. (2009) Fat. & Fract. Engng Mat. & Struct. **32**: 223-232
6. Gardin S., Courtin S., Bèzine G., Bertheau D. and Ben Hadj Hamouda H. (2007) Fat. & Fract. of Engng Mat.s & Struct. **30**: 231-242
7. Gardin S., Courtin S., Bèzine G., Bertheau D. and Ben Hadj Hamouda H. (2007) Fat. & Fract. of Engng Mat.s & Struct. **30**: 342-350
8. Walker K. (1970) In: Effects of environment and complex load history on fatigue life (Edited by Rosenfeld M.S.). ASTM STP 462: 1-14
9. Noda N. A. and Takase Y. (1999) Int. J. Fat. **28**: 151-163
10. Kalpakjian S. (Editor) (1991) Manufacturing processes for engineering materials, Adison-Wesley Publishing Company.
11. Atienza J.M. and Elices M. (2004) Mat. and Struct. **37**: 301-304
12. Elices M., Ruiz J. and Atienza J.M. (2004) Mat. and Struct. **37**: 305-310
13. Elices M. (2004) J. Mat. Sci. **39** : 3889-3899
14. Carpinteri A., Brighenti R., Vantadori S. (2006) Int. J. Mech. Sci. **48**: 638-649.
15. Carpinteri A. (1993) Int. J. Fat. **15**: 21-26
16. Carpinteri A., Brighenti R., Vantadori S., Viappiani D. (2007) Fat. & Fract. of Engng Mat.s & Struct. **30**: 524-534
17. Paris P.C. and Erdogan F.J. (1963) J. Basic Engng. **85**: 528–534
18. Iost A. (1991) Int. J. Fat. **13**: 25-33
19. Forman G.G., Kearney V.E. and Engle R.M. (1967) J. Basic Engng. **89**: 459–464
20. Ibrahim F.K. (1989) Fat. & Fract. of Engng Mat.s & Struct. **12**: 9-18
21. Zheng J. and Powell B.E. (1999) Int. J. Fat. **21**: 507-513
22. Mann T. (2007) Int. J. Fat. **29**: 1393-1401
23. Gurney T.R. (1979) Fatigue of Welded Structures. Cambridge Univ. Press, Cambridge.